

DEPENDENCE OF E-CLOUD ON THE LONGITUDINAL BUNCH PROFILE: STUDIES IN THE PS & EXTENSION TO THE HL-LHC*

C. M. Bhat[#], Fermi National Accelerator Laboratory, Batavia, IL, 60510, USA
H. Damerau, S. Hancock, E. Mahner, F. Caspers, G. Iadarola, T. Argyropoulos
and F. Zimmermann, CERN, Geneva, Switzerland

Abstract

Recent studies have shown that the prospects for significantly increasing bunch intensities in the LHC for the luminosity upgrade will be severely limited by the current cryo-heat capacity and the e-cloud (EC) driven beam instability. However, it is planned that during the HL-LHC era the bunch intensities in the LHC will go up by nearly a factor of two compared to the LHC-design values. Therefore, we may need to explore EC mitigation techniques that can be adopted in addition to those already in place. Preliminary simulations have indicated that long “flat” bunches can be beneficial over Gaussian bunches to reduce the EC build-up. Rigorous studies using realistic bunch profiles have never been done. Therefore, we have undertaken an in-depth investigation in the CERN 26 GeV PS to see if we can validate the previous findings and also if flattening the bunch can mitigate the EC. Here we present the results from dedicated EC measurements in the PS using varieties of bunch shapes and comparison with simulations. Finally, we make an extrapolation to the HL-LHC cases.

I. INTRODUCTION

Issues related to the e-cloud in lepton and hadron circular accelerators have become a serious problem for future high-intensity upgrades. The primary source of the e-cloud in these accelerators are interactions of the circulating charged particle beam with residual gas (i.e., by gas ionization) and/or by interactions of synchrotron radiation emitted by the circulating beam with the walls of the accelerator beam pipe. The former mechanism is relevant in medium energy hadron accelerators like CERN PS, SPS and Fermilab Booster and Main Injector etc. On the other hand, the latter mechanism plays a major role in many lepton accelerators and high energy hadron accelerators like the LHC.

Since the first identification of an e-cloud induced beam instability in 1965 and its cure by implementing a transverse feedback system in a small proton storage ring of the INP Novosibirsk by Budker and co-workers [1], significant research has been carried out at various accelerator facilities around the world [2-5] to understand the EC dynamics and on the possible mitigation techniques. Addressing the EC related issues has become one of the important topics for designing new high intensity accelerators and for upgrading the beam intensities in the existing accelerators.

The Large Hadron Collider (LHC) [6] at CERN came into full operation in early 2010. Over the past two years tremendous progress has been made from the point of view of its performance. The design goal of the LHC luminosity was $1 \times 10^{34} \text{ cm}^2 \text{ sec}^{-1}$ (with 25 nsec bunch spacing) at collision center of mass energy 14 TeV. Currently, the LHC has reached about 70% of its design luminosity even at 57% of its full energy. A staged approach for the luminosity upgrade has been planned for the High Luminosity LHC (HL-LHC) [7]. Two LHC bunch spacing: i) 25 nsec and ii) 50 nsec are under consideration. At the completion of the upgrades the peak luminosity (it is referred to as “peak virtual luminosity” in Table 1 of ref. [7]) is expected to be in excess of $20 \times 10^{34} \text{ cm}^2 \text{ sec}^{-1}$ and the bunch intensity up by a factor of two.

Currently, the LHC operates with a maximum of 1380 bunches with a bunch spacing of 50 nsec and intensities of about 1.5×10^{11} ppb. The experiments carried out during 2011-12 showed that the EC driven vacuum problem in the LHC [8] is one of the major limiting factors for 25 nsec bunch spacing. This is despite several EC mitigation measures like saw tooth pattern on the beam screen inside the cold dipole region, low secondary emission yield (SEY) NEG coatings on the inside surface of the beam pipe, etc. As a result, a major machine development campaign has been undertaken since 2011 to mitigate EC formation by beam scrubbing [9]. Consequently, significant improvement was seen [10] in the LHC performance. During the HL-LHC era the increased bunch intensity and the reduced bunch spacing will certainly elevate EC related problems. Therefore, it is highly recommended to search for novel methods which could be complementary to beam scrubbing and can be used in combination with others to reduce EC formation.

Early simulation studies in the LHC indicated that there is an anti-correlation between increased bunch length and the electron cloud formation; very long bunches with rectangular profile can reduce EC considerably [11]. But such bunches are presently not being considered for any of the LHC upgrade scenarios. On the other hand, an in-depth analysis using realistic but nearly flat short bunches suitable for the LHC was never been done. Therefore, a dedicated EC experiment has been carried out in the CERN PS at ejection momentum of 26 GeV/c and we investigated EC dependence on the form of the bunch profiles. Fitting the EC simulations to the measurement

data, we tried to study the correlation between bunch length and the EC evolution. Finally, we extended these studies to the HL-LHC scenario.

The high intensity bunches in the HL-LHC also have an additional issue related to single and multi-bunch instability driven by the loss of the Landau Damping [12]. Significant research has been carried out in the CERN SPS using its 4th harmonic rf system [13]. It has been concluded that a bunch shortening mode with higher harmonic rf system makes high intensity beam more stable. Consequently, adding an 800 MHz Landau cavity is foreseen to stabilize high intensity beam in the LHC during the HL-LHC era [14]. This implies that the peak line charge density in LHC bunches would go up, which may not be favourable from the EC point of view. Therefore, it is highly essential to examine the implications of the use of a higher harmonic rf system in the HL-LHC from the EC point of view.

Since 2007, the CERN PS has been equipped with a specially designed meter long EC monitor in the straight section (SS) 98 [15]. Figure 1 shows a schematic view of the detector. It has two identical 30 mm diameter button pickups on the upper part and a stripline-type electrode on the bottom of the vacuum chamber. The pickup detectors are shielded differently: BPU1 and BPU2 use 0.7 mm thick perforated stainless steel sheets (providing $\approx 10\%$ transparency) and two grids (providing $\approx 37\%$ and 23% transparency), respectively.

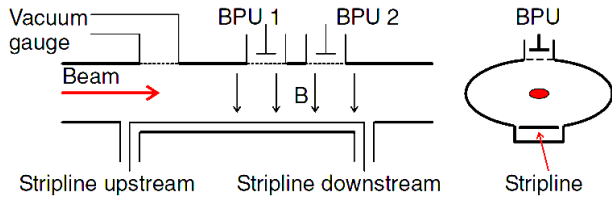


Figure 1: Schematic of the EC detector used in the PS straight section (SS) 98 (courtesy of E. Mahner [15]).

Clear EC signals and correlated vacuum degradation have been observed. The EC buildup has been observed only on the 25 nsec bunch spacing LHC25 cycle and mainly for the last 36 ms before the beam ejection from the PS. Figure 2(a) shows the measured cumulative electrons from each pickup together with the vacuum pressure readings. Figure 2(b) shows typical PS mountain range [16] data during the last 140 ms on the same PS cycle. Figure 2(c) shows stages for rf turn-on times on the cycle (at flat-top) during the quadrupole-splitting of the beam to finally produce a train of 72 bunches with 25 nsec bunch spacing. E. Mahner and his co-workers [15] have also deduced a transfer function between measured signals from the detectors and the electron line-density using system impedance, button transparencies etc.. They found that the relation between electron line density and button pickup voltage U_{BPU1} , is $\lambda/(e^{\prime}/m) = 2.3 \times 10^8 (U_{BPU1}/mV)$.

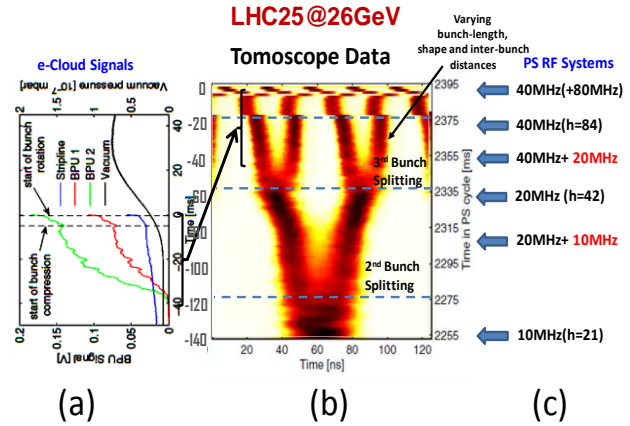


Figure 2: The region of interest from EC point of view in the PS beam on the LHC25 cycle[15] (for four bunches out of seventy two). (a) Measured EC signals from BPU1 (red curve), BPU2 (green curve) and stripline (blue curve) detectors along with vacuum (black curve) (b) mountain range data of the PS beam using tomoscope, and (c) used PS rf systems for beam quadrupole splitting.

On the flat-top of the LHC25 cycle the bunch profile takes varieties of shapes and a range of bunch lengths. For example, at 40 ms before the ejection, the 4σ bunch length is about 15 nsec as shown in Fig. 3. During the final double splitting at about 60 ms before ejection, dramatic bunch profile variation takes place in the double harmonic rf bucket made up of $h=42$ and $h=84$ rf systems. Eventually, an adiabatic bunch compression followed by a rapid bunch rotation (which is a quasi-nonadiabatic process) in a combined $h=84$ and $h=168$ rf bucket shorten the bunches to final length < 4 nsec at extraction. A very large growth in EC buildup has been seen as the bunch rotation was taking place (see Fig. 2(a)). Fortunately, this spike in the EC density does not seem to have much detrimental effect on the PS beam because it is ejected exactly at this point on the cycle.

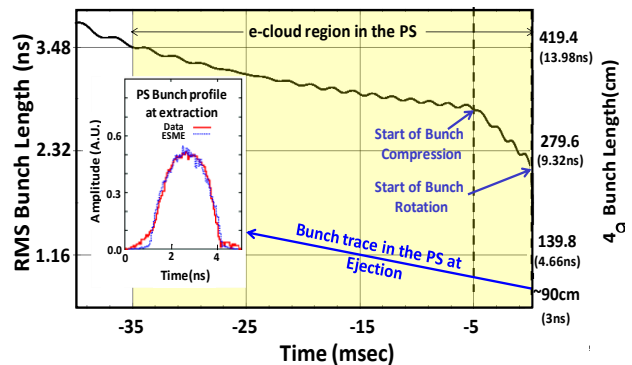


Figure 3: RMS bunch length variation during the last 40 ms on the PS-LHC25 beam cycle. The measured bunch profile just before ejection from the PS and its comparison with the predicted bunch profile using ESME is shown in the inset.

We realized that one can exploit the flexibilities of the PS in terms of rf system to study the EC effect on the bunch lengthening mode (BLM) and bunch shortening mode (BSM) under a controlled environment by the changing bunch shapes adiabatically. And conduct in-depth EC simulation study using the measured data to benchmark the available EC simulation codes.

This paper is organized in the following way. We first give a brief review on the EC simulation codes used in the present analyses. In Sec. III, we discuss the dedicated EC experiment in the PS and the data analysis. Sec. IV describes the EC simulation effort for the HL-LHC operating scenario. In the final section we summarize our findings.

II. E-CLOUD SIMULATIONS

The EC simulations have been carried out using ECLLOUD [17] and a newly developed code PyECLLOUD [18]. Both ECLLOUD and PyECLLOUD use the same EC model, but the latter code uses faster algorithms and incorporates a few improvements. Both of these codes simulate EC cloud buildup when a train of bunches is injected into an empty accelerator section. The model adopted in both of these codes assumes that the total SEY, δ_{tot} , is a sum of two quantities i) true SEY and ii) a component arising from elastic reflection given by [3 (refer to an article by F. Zimmermann, page 14), 4, 19],

$$\delta_{\text{tot}}(E_p, \theta) = \delta_{\text{true}}(E_p, \theta) + R0 \delta_{\text{Elastic}}(E_p) \quad (1)$$

where,

$$\delta_{\text{true}}(E_p, \theta) = \delta_{\text{Max}}^*(\theta) \frac{sE_p / \varepsilon_{\text{Max}}(\theta)}{s - 1 + [E_p / \varepsilon_{\text{Max}}(\theta)]^s} \quad (2)$$

$$\delta_{\text{Max}}^*(\theta) = \delta_{\text{Max}}^* \exp\left[\frac{1}{2}(1 - \cos(\theta))\right] \quad (3)$$

$$\varepsilon_{\text{Max}}(\theta) = \varepsilon_{\text{Max}}^* [1 + 0.7(1 - \cos(\theta))] \quad (4)$$

$$\delta_{\text{Elastic}}(E_p) = \left(\frac{\sqrt{E_p} - \sqrt{E_p + E_0}}{\sqrt{E_p} + \sqrt{E_p + E_0}} \right)^2 \quad (5)$$

In the above equations the quantities E_p , δ_{true} , δ_{Elastic} , δ_{Max} , ε_{Max} , $R0$ and θ , are the incident electron energy, parameterized secondary emission yield from the measurement data, E_p -dependent elastic reflectivity ($\delta_{\text{Elastic}} \rightarrow 1$ as $E_p \rightarrow 0$), maximum of δ_{true} , electron energy at δ_{Max} , probability for elastic reflection in the limit of zero primary energy of electrons, and angle of incident of the primary electrons (with $\theta=0$ taken as perpendicular impact), respectively, with $E_0=150$ eV and $s \approx 1.55$ (a value of 1.35 is suggested for fully conditioned copper [19]). The quantity $R0$ (in the range of 0 to 1) in this model accounts for a memory effect for the trapped electrons even after the bunch train has passed by. In other words, the observed EC buildup during the passage

of a bunch is enhanced by the passage of a preceding bunch.

For most of the cycle the measured EC buildup in the PS experiment [15] was at its steady-state condition (because, the rf manipulation was relatively slow compared to the EC growth and its decay per passage), except during the fast bunch rotation. In order to guarantee that a steady-state condition is reached in our simulated EC buildup, it was necessary to carry out calculations for multiple passage of the PS bunch train taking into account the filling pattern, kicker gap and details of bunch profiles. In our simulations, we had to go up to twenty passages for the same beam through the EC detector. (We explain this aspect of the simulations in detail in Sec. III).

Table 1: PS machine and EC parameters used in the ECLLOUD and PyECLLOUD simulations. The best values of SEY are highlighted.

Parameters	Values
Proton Momentum	26 GeV/c
Number of Bunches/turn	72
Bunch Intensity	1.35E11ppb
Bunch spacing	Varying (25-50nsec)
Bunch Length (4 σ)	Varying in the range of 3-33 nsec
Bunch Shape/Profiles	Varying shapes
Kicker Gap	0.3 μ s
Beam Pipe: H and V Aperture (half)	7.3cm(H), 3.5cm(V)
Material of the Beam Pipe	Stainless Steel 316 LN
Beam Transversers Emit. $\varepsilon_x=\varepsilon_y$	2.1 μ m
Lattice Function at the Detector β_x and β_y =	22.14 m, 12.06 m
Ionization Crosection	1 and 1.5 Mbarn
Gas Pressure	10 nTorr
Maximum SEY yield δ_{Max}	1.57 (Varied between 1.3-1.7)
R0: Probability for Elastic Reflection in the Limit of Zero Primary Energy of Electrons	0.55 (Varied between 0.3-0.7)
Electron Energy at δ_{Max} (eV)	287 (Varied bewteen 230-332)

Table 1 lists the EC simulation parameters for the PS. Primary seed electrons are assumed to be produced by gas ionization. We varied the gas ionization cross section by about +50% in our simulations to investigate its effect on the saturation values of EC line-density. The study showed that the EC saturation value has little dependence (<1%) on the range of ionization cross section considered here. The PS EC detector consists of an elliptical 316LN (low carbon with nitrogen) stainless steel chamber. Test-bench measurement data on the 316LN stainless steel [20] has been used to fit a non-linear curve given by Eq. 2 which gave $\delta_{\text{Max}}^* = 1.85$, $\varepsilon_{\text{Max}}^* = 282$ eV and $s=1.55$. These values seems to be too pessimistic, because one can expect a significant reduction in the total SEY due the several years of beam scrubbing on the PS during its normal operation. Therefore, we have carried out simulations searching for a somewhat reduced δ_{Max}^* in the range of 1.3 to 1.7, which best represents our data.

The EC simulations for the HL-LHC have been carried out only at the proton beam energy of 7 TeV and we assume that the primary seed electrons are exclusively from the synchrotron radiation induced photo-emission off the inner side of the beam pipe. In the model [19],

Table 2: HL-LHC machine parameters and EC parameters used in the ELOUD and PyELOUD simulations.

Parameters	Values
Proton Energy	7000 GeV
Number of Bunches/turn	2808 @ 25nsec bunch spacing 1404 @ 50nsec bunch spacing
Bunch Intensity	2.2E11ppb @ 25nsec bunch spacing 3.5E11ppb @ 50nsec bunch spacing
Bunch spacing	25 and 50nsec
Bunch Length (4σ)	Varying in the range of 0.9-1.33 nsec
Bunch Shape/Profiles	Varying shapes
Kicker Gap	200nsec
Beam Pipe: H and V Aperture (half)	2.2cm(H), 1.73cm(V)
Material of the Beam Pipe	TiZrV Non-evaporable Getter (NEG) Coated
Beam Transvers Emit. $\epsilon_x=\epsilon_y$	2.5 μm for 25 nsec bunch spacing 3.0 mm for 50 nsec bunch spacing
Lattice Function at the Detector β_x and β_y	86.37 m, 92.04 m
Source of primary electrons & Reflectivity	100% Photo emission 20%
Primary electron emission yield	0.00087
Reflected electron Distribution	$\cos^2\psi$
Maximum SEY yield δ_{Max}	1.3 to 1.7
R0: Probability for Elastic Reflection in the Limit of Zero Primary Energy of Electrons	0.2 t 0.7
Electron Energy at δ_{Max} (eV)	239.5

about 80% of the photons produce photo-electrons on first impact with the beam pipe. All of these electrons lie in a narrow cone of 11.25° and will never get accelerated by the proton beam. Consequently, they will not contribute to further EC buildup. On the other hand, the electron produced by the rest of the 20% of the photon flux will get distributed azimuthally according to $\cos^2\psi$ and contribute to the further to EC buildup in the LHC.

III. PS E-CLOUD MEASUREMENTS

Experiment

The current PS e-cloud measurements have been made using the PS EC detector and the PS beam cycle similar to the operational LHC25 cycle. Until 5 ms before beam extraction the rf manipulations have been kept unchanged. By this time, the final train of 72 bunches with 25 nsec bunch spacing was fully formed. The rf voltage of the 40 MHz rf system was programmed to be at 40 kV. Then new rf manipulation sequences have been adopted as shown in Fig. 4(a). The 80 MHz rf system was turned on with the rf phase either at 0° (in phase) or 180° (counter phase). From here on, five different iso-adiabatic bunch manipulation schemes have been followed. 1) SH: voltage on the 40 MHz rf system has been increased linearly from 40 kV to 100 kV, keeping the 80 MHz rf system turned off. This left the bunches in a single harmonic rf bucket and the bunches were continuously being shortened for the next 5 ms (black

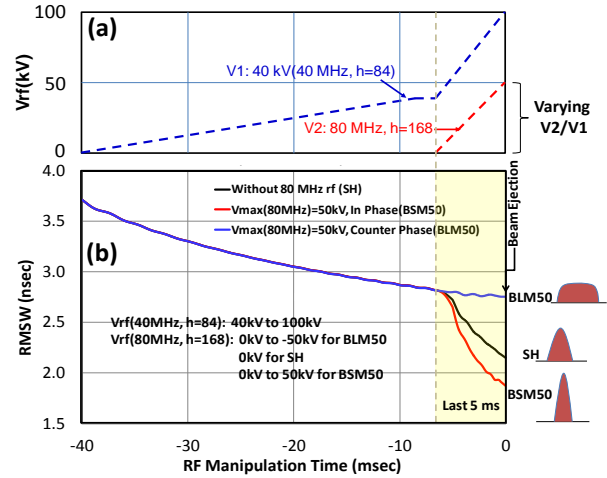


Figure 4: (a) PS rf manipulation and (b) ESME predicted bunch length variation during the last 40 ms before beam ejection. Until the last 35 ms the rf manipulations are identical to the those of the operational cycle that produces bunches with 25 nsec spacing. During the last 5 ms, the 40 MHz and 80 MHz rf systems are ramped up simultaneously and linearly, to final values of 100kV and 50 kV, respectively.

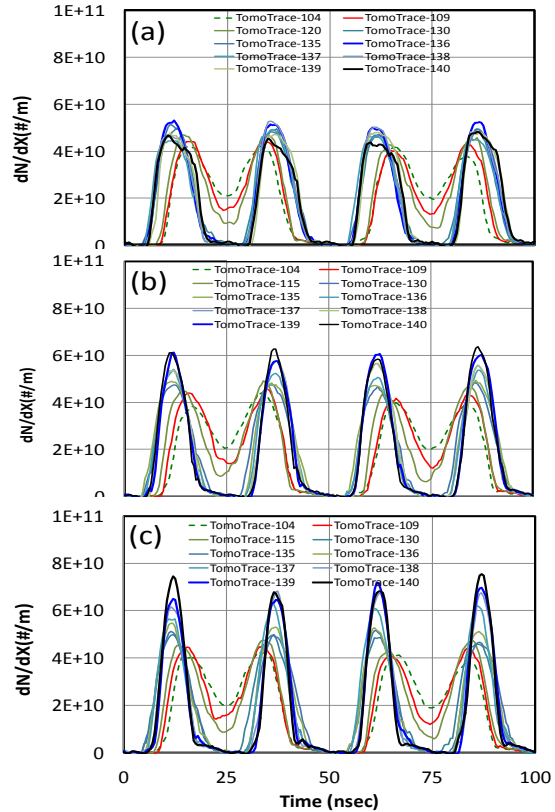


Figure 5: PS bunch profiles during the last 40 ms of the rf manipulations for a) BLM50, b) beam in $h=84$ rf buckets (SH) and c) BSM50 for four bunches out of 72. In these cases, the bunch rf manipulations differ only during the last 5 ms. The trace numbers in the figure indicate relative time in the PS cycle (see Table 3).

curve in Fig. 4(a)). 2) BSM50: the 40 MHz and 80 MHz rf systems have been ramped up simultaneously in phase from 40 kV to 100 kV and 0 kV to 50 kV, respectively. Here the beam has been maximally squeezed giving rise to the shortest bunch and the final value of $V_2(80\text{MHz})/V_1(40\text{MHz})=0.5$. 3) BSM25: similar to “2” but 80 MHz system ramped only up to 25 kV, 4) BLM25: similar to “3” but, rf systems in counter phase and 5) BLM50: similar to “2” but, rf systems in counter phase. This led to nearly “flat” bunches which results from $V_2(80\text{MHz})/V_1(40\text{MHz})=-0.5$.

Figure 4(b) shows the simulated RMS bunch lengths in the PS for the entire rf cycles of interest using the longitudinal beam dynamics code ESME [21]. It is important to note that the rf voltage ratios $V_2(80\text{MHz})/V_1(40\text{MHz})$ were varying from zero to a set final value of ± 0.50 during the rf manipulation period until the beam got ejected. Ideally, we wanted to hold the beam at the final values of the voltage ratios for an extended period. But the operational constraints on the LHC25 cycle existed at the time of the experiment prevented us.

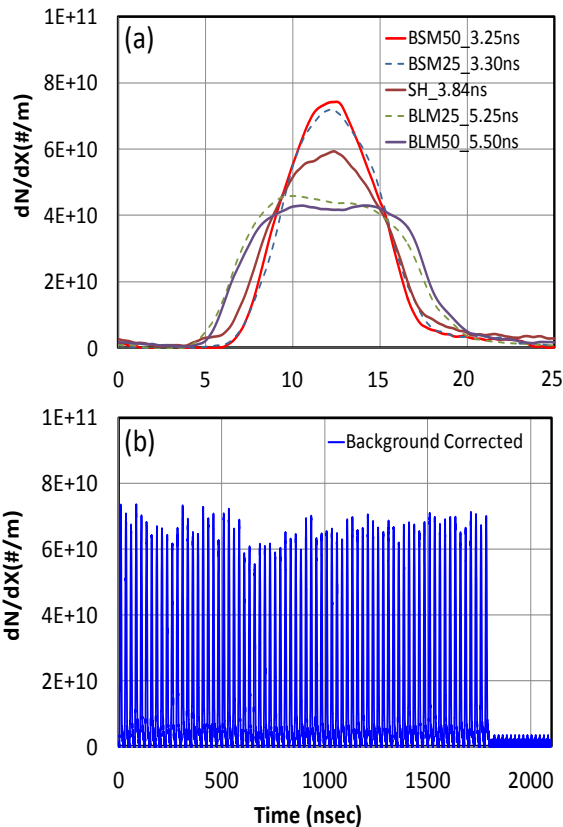


Figure 6: Typical PS bunch profiles at ejection for a) all five cases studied here b) entire train of 72 bunches (after background correction). The single bunch intensity was about 1.35×10^{11} ppb in all the cases shown here.

Figure 5 shows the measured bunch profiles using the PS Tomoscope application for the region where EC buildup is observed. The total PS beam intensities for the three cases shown here were 980E10, 985E10 and

973E10 for BLM50, SH and BSM50, respectively. The average final bunch population was about 20% larger than that used in ref. 15. A total of 140 traces with delay of 480 PS revolution periods from trace to trace were recorded. The trace number and the corresponding time on the PS cycle relative to the beam ejection are listed in Table 3. Data show that the general features for all of the traces from 104 to 135 for three different cases resemble each other except for a small difference arising from the beam intensity variation ($<1\%$). The Trace135 to Trace140 correspond to the last 5 ms and bunch profiles for these three cases differ significantly. The measured RMS transverse emittance (using wire scanners) was about $2.1 \mu\text{m}$.

Table 3: Trace number versus time relative to the beam ejection from the PS. These are referred to in Figure 5.

Trace	Time Relative to PS Beam Ejection (ms)	Comments
Trace104	-36.24	Background
Trace109	-31.21	Start of EC
Trace115	-25.17	Growth pt.(Mid)
Trace120	-20.13	\approx Stable EC
Trace130	-10.07	Same as Above
Trace135	-5.03	40MHz \oplus 80MHz
Trace136	-4.03	“
Trace137	-3.02	“
Trace138	-2.01	“
Trace139	-1.01	“
Trace140	0	“

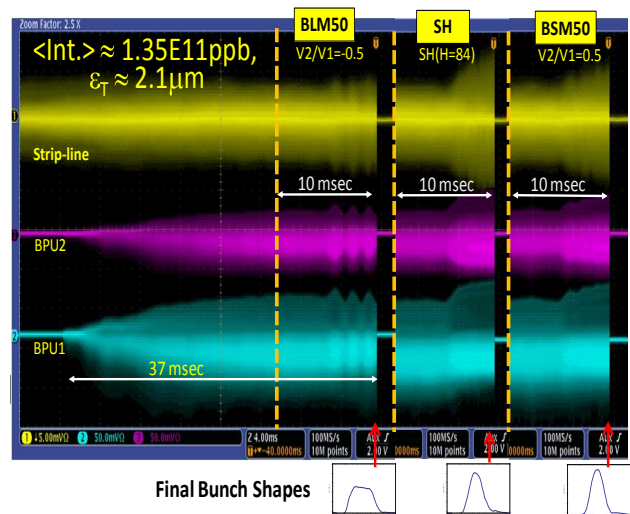


Figure 7: Signals from the EC monitor from three different detectors viz., strip-line, BPU1 and BPU2 for three rf manipulation scenarios. The bunch shapes at ejection are also shown.

Figure 6(a) displays typical bunch profiles at beam ejection for all five cases studied here. The RMS bunch lengths in each case have also been listed for comparison. Figure 6(b) shows a typical PS bunch train of 72 bunches at ejection. The bunch to bunch intensity variation was $<10\%$.

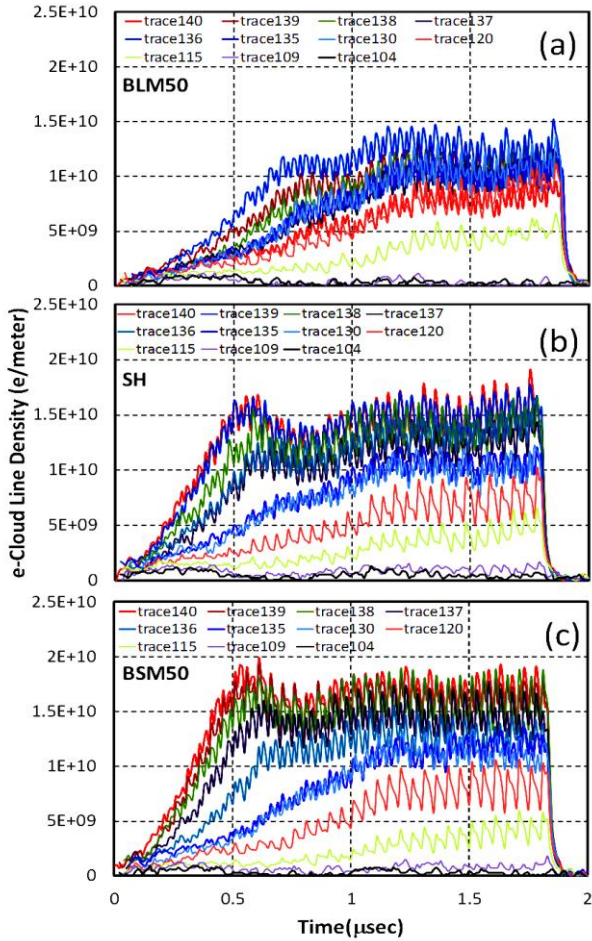


Figure 8: EC line-density measured on different time of the PS cycle during the last 40 ms before the beam ejection. The data shown from BPU1 are for a) BLM50, b) SH and c) BSM50. Notice that the EC behaviour was similar till trace130. But, they differ significantly from trace130 (also see Fig. 10 for Trace140).

Figure 7 shows typical EC monitor scope data for the last 37 ms on the PS cycle for BLM50 and data for the last 10 ms for SH and BSM50 cases. Figure 8 shows EC line-density measured from BPU1 for each of the PS turns corresponding to bunch profiles shown in Fig. 5. One can see a clear difference between the EC growth for BLM50 and the other two cases only during the last 5 ms. The data show that growth and saturation values strongly depend on the bunch profiles. However, independent of their peak electron-line density each one will decay in about 0.1 μsec after passage of the last bunch. Since the rf manipulations are sufficiently slow (i.e., the incremental change in bunch profile is almost negligible for a number of passages through the EC detector region

as compared with EC growth and decay time, unlike in the case of fast bunch rotation mentioned in Sec. I), one can assume that the EC line density has reached a steady state in all cases shown in Fig. 8.

EC Simulations and Comparison with the Data

Initially, the simulation studies of the measured EC buildup in the PS have been carried out using the code ECLLOUD. The original version of the code could handle only standard Gaussian bunch profiles with a few non-standard shapes like flat, trapezium shapes etc. Also, there were issues related to adopting a non-standard filling pattern. The code has thus been modified to incorporate complex bunch profiles including a non-standard bunch filling pattern. In the meanwhile, PyECLLOUD became available which could accommodate both standard as well as non-standard bunch profiles. All the simulation results presented here for the PS cases use the PyECLLOUD code.

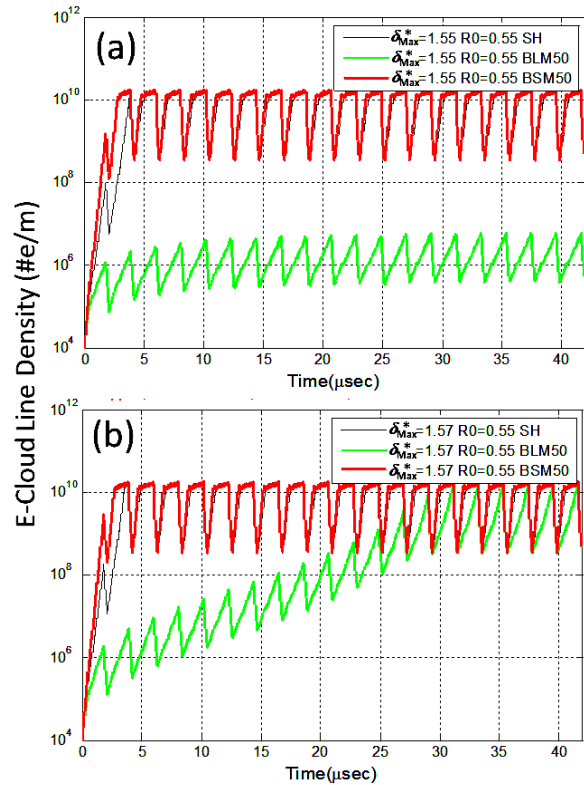


Figure 9: PS EC simulations using PyeCLOUD with $\mathcal{E}_{Max}^* = 287$ eV and a) $\delta_{Max}^* = 1.55$, $R0=0.55$ b) $\delta_{Max}^* = 1.57$, $R0= 0.55$ (optimized). Calculations are carried out for the drift section of the PS EC detector. These two cases are shown as examples to illustrate combined sensitivity of EC growth on SEY parameters and bunch shapes.

Starting from the measured values of $\delta_{Max}^* = 1.85$ and $\mathcal{E}_{Max}^* = 282$ eV for the 316LN stainless steel, we scanned the SEY parameter space (see Table 1). All of our simulations take the exact bunch profiles into account (shown in Fig. 5) with bunch to bunch intensity variation similar to that shown in Fig. 6(b) and the measured beam

intensity in the PS. Figure 9 illustrates an example of such simulation results for two sets of SEY parameters and for three different beam profiles at ejection. The black, green and red curves are for SH, BSM50 and BLM50 cases, respectively. For the cases shown in Fig. 9(b) the steady state was reached with about fifteen passages of the PS beam. In all of our simulations we allowed up to 20 passages. These simulations clearly show the sensitivity of the EC buildup on the bunch profile and the SEY parameters. In the case illustrated here, we observe about four orders of magnitude change in EC the line density for a 2% change in δ_{Max}^* for BLM50 to BSM50. This suggests that one could possibly use the bunch profile dependence of EC growth to estimate the SEY quite accurately.

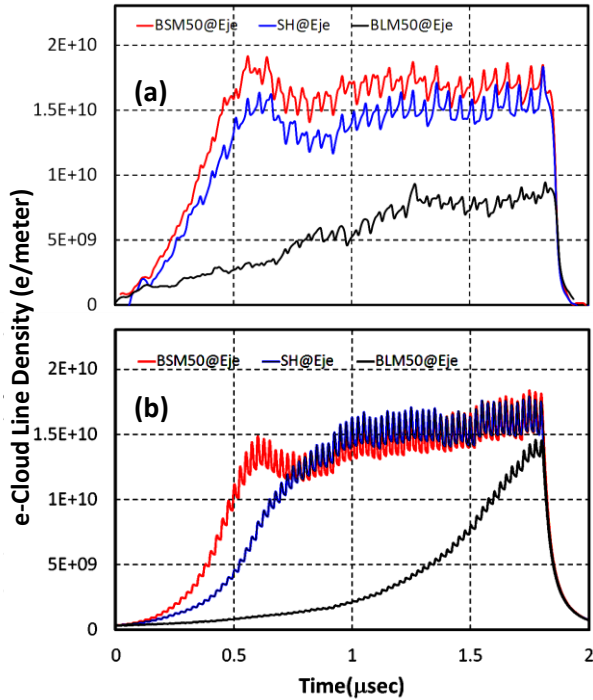


Figure 10: (a) Measured EC line-density in the PS at ejection and (b) the PyECLLOUD simulation results corresponding to the cases shown in “a”. The simulations have been carried out using high-lighted parameters in Table 1.

Figure 10 displays a comparison between the measured and the simulated e-cloud line-density using $\varepsilon_{Max}^* = 287$ eV, $\delta_{Max}^* = 1.57$ and $R0 = 0.55$ for the ejection traces. There is no normalization between the simulation results and the measurement data. We find quite good agreement between the saturation values for the BSM50 and SH cases. Also, the overall trend is well reproduced. In the case of BLM50 the quality of agreement is not that satisfactory. The simulated EC line density grows rather slowly initially and reaches a steady state maximum at about 30% larger than the measurement value in the case of BLM50. In any case, the predicted cumulative

electrons are within the 30% of the measured value of $3E12$ electrons for the BLM50.

Next, the simulations have been carried out using the same set of SEY parameters, mentioned above, to predict the complete EC buildup measured in the experiment. Figure 11 presents measured cumulative electrons per PS turn versus the relative time on the PS cycle. An error of 10% is assigned to the measured data points which include a systematic error and a background subtraction error. The overlaid three curves represent simulation results with a normalization factor of 0.85. The overall trend of the cumulative electrons is predicted quite well in all three cases. Simulations are found to reproduce even the observed oscillations during the last 5 ms in the case of BLM50. However, for SH and BSM50, the accumulated electrons on the last turn of the beam in the PS are underestimated by 25% and 50%, respectively, in the simulations.

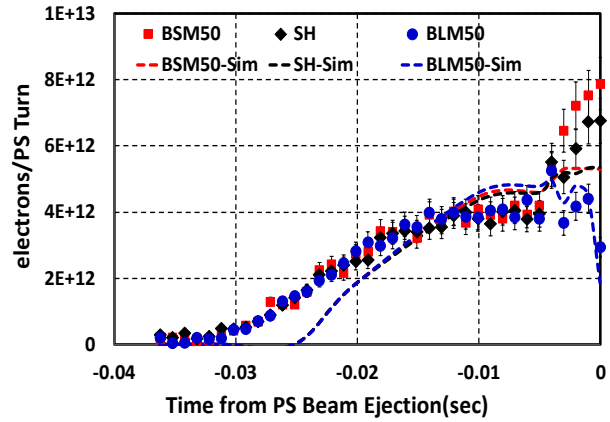


Figure 11: Overlay of the measured (red square – BSM50, dark diamond– SH, and blue circles – BLM50) cumulative electrons/PS turn and their predictions using PyECLLOUD. The relative normalization between simulations and measured data is 0.85.

From the PS study we clearly observe a dependence of EC growth on the bunch profile. We find that the ratios $BSM50/BLM50 \approx 2.7 \pm 0.4$ and $SH/BLM50 \approx 2.3 \pm 0.3$ for the measured cumulative electrons at ejection. Certainly BLM gives rise to considerably smaller EC buildup compared to other cases. A comparison between measurements and the simulations sets a tight range of values on the SEY parameters for the PS EC detector region. For example, we found $\varepsilon_{Max}^* = 287$ eV ($\pm 3\%$), $\delta_{Max}^* = 1.57$ ($\pm 8\%$) and $R0 = 0.55$ ($\pm 3\%$). Also, we have been able to benchmark the EC simulation codes and the used SEY model quite satisfactorily.

IV. E-CLOUD IN THE HL-LHC

Over the last decade significant research has been carried out on the LHC EC issues [2-5, 8, 9, 19, 22 and 23]. Most of the presented simulation studies assume Gaussian bunch profiles and bunch intensities close to the

LHC design values [6]. A lot of effort has been put to scan SEY parameter space. Ref. 19 presents EC-simulation results for the higher intensity operation of the LHC including some simulations for the flat bunch profiles. All of them have used about 25% and 50% larger transverse emittances on the 25 nsec and 50 nsec bunch filling patterns, respectively, as compared to the HL-LHC specifications (see also Table 4). However, the EC is a very complex, non-linear multi-dimensional phenomenon. Further, the SEY parameters change for better with machine operation. As a result of this, it is practically impossible to foresee every issue that one might encounter. Therefore we focus our study on using realistic bunch profiles and better established SEY parameters.

Table 4: HL-LHC parameters of interest for EC issues [7]

Parameter	nominal	25ns	50ns
N	1.15E+11	2.2E+11	3.5E+11
n_b	2808	2808	1404
beam current [A]	0.56	1.12	0.89
x-ing angle [μ rad]	300	590	590
beam separation [σ]	10	10	10
β^* [m]	0.55	0.15	0.15
ϵ_n [μ m]	3.75	2.5	3.0
ϵ_L [eVs]	2.51	2.5	2.5
energy spread	1.20E-04	1.20E-04	1.20E-04
bunch length [m]	7.50E-02	7.50E-02	7.50E-02
IBS horizontal [h]	80 -> 106	2.54	2.66
IBS longitudinal [h]	61 -> 60	15.8	13.2
Piwinski parameter	0.68	3.12	2.66
geom. reduction	0.83	0.31	0.33
beam-beam / IP	3.10E-03	3.9E-03	5.0E-03
Peak Luminosity	1×10^{34}	7.4×10^{34}	8.5×10^{34}
Beam Brightness (R.U.)	1	2.9	3.8
Pileup $L_{level}=5L_0$	19(27)	140	140

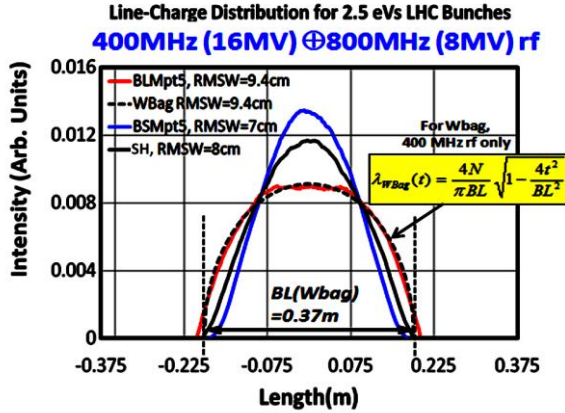


Figure 12: (ESME) Simulated HL-LHC beam bunch profiles in double harmonic rf buckets for BLM50 (BLMpt5), Waterbag, BSM50 (BSMpt5) and SH (in 400 MHz rf bucket).

Currently, the LHC is not instrumented with EC monitors as in the case of the PS and the SPS at CERN. All the information related to the EC in the LHC is deduced from the measured vacuum activities in various sectors of the ring. Recently, a stringent range of SEY parameters has been deduced [10] by using the 2011-12 vacuum data in the uncoated warm regions of the LHC

and comparing it with ECLLOUD simulations. $\epsilon_{Max}^* = 239.5$ eV and $\delta_{Max}^* < 1.55$ have been recommended. Here, we study the EC for the LHC using the HL-LHC beam parameters and the new values of SEY for varieties of possible realistic bunch profiles with a goal of investigating if a particular bunch profile is better than another from the point of view of EC mitigation.

Figure 12 shows ESME-simulated bunch profiles for the LHC. Guided by the measurements on the bunch profiles in the LHC at 4 TeV, we have used a Hoffman-Pedersen (elliptical) distribution for the beam in 400 MHz rf buckets at 7 TeV. An rf voltage of 16 MV is assumed. The profiles BSMpt5 and BLMpt5 have been generated by superposing the 2nd harmonic (800 MHz) rf wave on the fundamental rf wave of 400 MHz with $V2/V1 = \pm 0.5$, respectively. The dashed dark curve corresponds to the bunch profile from a “water-bag” (constant beam particle density distribution in the longitudinal phase space) model [24].

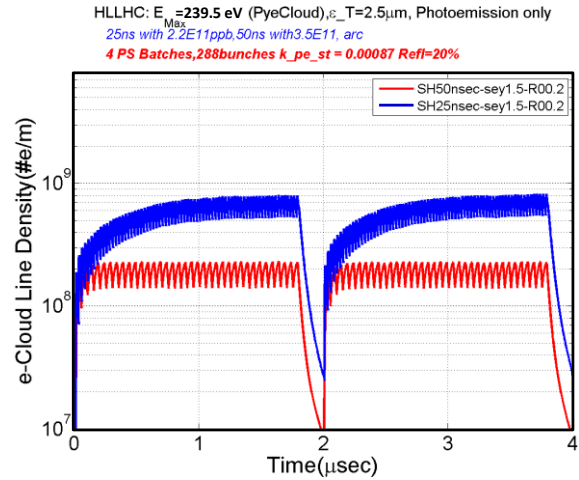


Figure 13: PyeCLOUD simulations with $\epsilon_{Max}^* = 239.5$ eV, $\delta_{Max}^* = 1.5$, $R0=0.2$ for the HL-LHC beam parameters. Red and blue curves are for 3.5×10^{11} ppb with 50 nsec bunch spacing and 2.2×10^{11} ppb with 25 nsec bunch spacing, respectively. SH bunch profile is used in these simulations. For clarity, both of these curves are smoothed and results for only two PS batches are shown.

EC simulations have been carried out with ECLLOUD as well as the PyECLLOUD using the parameters listed in Table 2 and 4. We have also extended some of the simulations for intensities in the range of $1-4 \times 10^{11}$ ppb. The current simulation uses the best known values of $\epsilon_{Max}^* = 239.5$ eV and δ_{Max}^* in the range 1.3 to 1.7 and $R0$ in the range of 0.2 to 0.7. (Measured values of δ_{Max}^* for the NEG was in the range of 1.1 to 2.0[25]). We have used a standard SPS batch of 288 bunches (similar to one in original LHC design) made of four batches from the PS (see for example Fig. 6(b)) each separated by 200 nsec.

The individual bunch profile was similar to those shown in Fig. 12. For all values of SEY parameters used in our simulations, a clear signature of a steady state is seen by the end of the passage of the first PS batch as shown in Fig. 13. The SH profile has been used in both cases in this figure. Preliminary results from a similar EC simulation for the LHC with different bunch profiles generated using a double harmonic rf system have been reported earlier [26]. The electrons from EC, ultimately deposit their energy on the beam pipe. Heatload on the LHC cryo-system comes from the absorbed energy from the beam pipe.

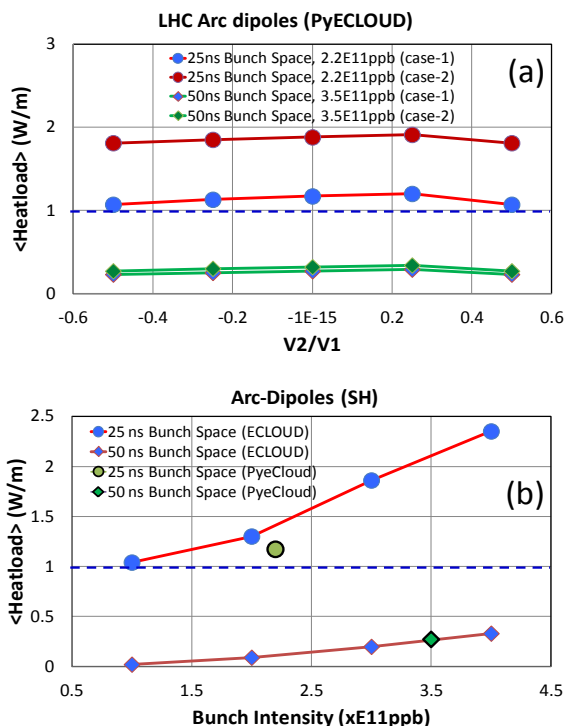


Figure 14: Calculated average heatload for the HL-LHC beam scenarios: a) bunch profile dependence (left-most points are for BML50 and rightmost points are for BSM50, the points at $V2/V1 = 0$ are for the SH). “case-1” implies $\delta_{Max}^* = 1.5$, $R0 = 0.2$. “case-2” implies $\delta_{Max}^* = 1.5$, $R0 = 0.5$. b) Bunch intensity dependence (– simulations are performed with “case-1” sey parameters). PyECLoud simulations results are also shown for comparison. The blue dashed line represents the heat load capacity of the existing LHC cryo-system.

Cryogenic superconducting dipoles in the LHC occupy about 66% of the ring and carry the majority of the cryo-heat load. Therefore here we concentrate all of our simulations on the LHC dipoles (arcs). The calculated heatload for various bunch profiles and two sets of SEY are shown in Fig. 14(a) and the heatload dependence on the bunch intensity is shown in Fig. 14(b). The contributions from quadrupoles and other cryo magnets to the total heatload are ignored here. The EC simulations on arcs clearly show that the headload has very little dependence on the bunch profiles. Therefore, BLM can

not be used as an EC mitigation technique in the LHC. The observed difference between PS and the LHC EC dependence on the bunch profiles may be primarily due to significantly shorter bunches in the LHC; the LHC bunches are about an order of magnitude smaller than those studied in the PS. For example, the shortest bunch in the PS (in our experiment) has bunch-length (4σ) ≈ 13 nsec, while, that in the LHC, the longest bunch studied has bunch-length (4σ) ≈ 1.3 nsec. Consequently, LHC bunches are too short to have any profile dependence on the EC growths. This needs further studies.

Simulations show that even for the most pessimistic case of $\delta_{Max}^* = 1.7$, $R0 = 0.7$ (from Table 2) the average heatload <0.5 W/m in the case of the 50 nsec bunch filling pattern. On the other hand, the calculated heatload for any of the 25 nsec bunch filling patterns is more than the design heatload handling capacity of the LHC cryo-system (shown by the dashed blue curves in Fig. 14) if $\delta_{Max}^* \geq 1.5$. Therefore, upgrades to the LHC cryo-system are inevitable for future operation with the 25 nsec bunch spacing at higher intensities unless the SEY is reduced significantly from the current known values. The present simulations show that the LHC filling pattern with 50 nsec bunch spacing has a clear advantage over the 25 nsec bunch spacing even during the HL-LHC era.

The fact that the EC buildup has little dependence on the bunch profiles in the LHC bodes well for the foreseen rf upgrades during HL-LHC era. The high intensity beam can be made stable by use of a 2nd harmonic Landau cavity if the bunches are in the BSM (or BLM mode for longitudinal emittance below some threshold). From the current analysis, we show for the first time that the use of a Landau cavity in the LHC will have negligible effect on the EC growth.

V. SUMMARY

During the HL-LHC era the beam intensity in the LHC is expected to go up at least by a factor of two. This has direct implications on the EC growth and the issues related to the beam instability driven by the dynamics of the electron cloud. Therefore it is important to explore and develop techniques to mitigate EC growth. Fully developed techniques like NEG coatings on the inner surface of the beam pipe and a saw tooth pattern on the beam screen inside the cold dipole region have been adopted in the LHC. Many new techniques are under consideration.

Early EC simulations have shown that the flat bunches have advantages over Gaussian bunches. In this regard, we conducted an EC experiment in the PS at its extraction energy where the EC is observed and the bunch profiles change significantly. Exploiting PS rf capabilities, varieties of required bunch profiles, including nearly flat bunches, have been generated and EC growth is studied. Using the available EC codes at CERN, simulations have been carried out incorporating the measured PS bunch profiles. There was a good agreement between the EC measurements and the simulation results. These studies

enabled us to determine the SEY parameters for the EC monitor region of the PS quite accurately; we found that $\varepsilon_{Max}^* = 287 \text{ eV} (\pm 3\%)$, $\delta_{Max}^* = 1.57 (\pm 8\%)$ and $R0 = 0.55 (\pm 3\%)$. We also find that the nearly flat (BLM50) bunches produce about a factor 2.7 ± 0.4 lower number of electrons than Gaussian bunches.

We have then extended similar studies to the HL-LHC beam conditions through simulations, where the bunch lengths were nearly ten ($3.25 \text{ nsec(PS)}/0.31 \text{ nsec(LHC)}$) times smaller than that in the PS at extraction. We found that the EC growths are almost independent of bunch profiles. Consequently, the foreseen installation of a second harmonic Landau cavity, that would change bunch profiles to BSM and make the beam longitudinally more stable, will not pose any additional EC related problems in the LHC.

ACKNOWLEDGMENT

The authors would like to thank the CERN operation team for their help while conducting the beam experiments in the PS accelerator. One of the authors (CMB) is specially indebted to F. Zimmermann, O. Brüning, G. Arduini, E. Shaposhnikova, R. Garoby, G. Rumolo and S. Gilardoni for their hospitality at CERN and many useful discussions. Also, special thanks are due to Humberto M. Cuna for his help in early stages of simulation studies and, M. Goodman for his comments on this paper. This work is supported by Fermi Research Alliance, LLC under Contract No. DE-AC02-07CH11359 with the U.S. Department of Energy, US LHC Accelerator Research Program (LARP) and Coordinated Accelerator Research in Europe – High Intensity, High Energy, Hadron Beam (CARE-HHH).

REFERENCES

[1] G. Budker, G. Dimov, and V. Dudnikov, in *Proceedings of the International Symposium on Electron and Positron Storage Rings, Saclay, France, 1966* (Saclay, Paris, 1966), Article No. VIII-6-1.

[2] F. Zimmermann, *Phys. Rev. ST Accel. Beams* 7, 124801 (2004).

[3] “Electron Cloud Effects in Accelerators”, edited by K. Ohmi and M. Furman (2004), *ICFA Beam Dynamics Newsletter*, Vol.33 April 2004, p 14-156.

[4] R. Cimino, I. R. Collins, M. A. Furman, M. Pivi, F. Ruggiero, G. Rumolo and F. Zimmermann, *Phys. Rev. Letts.* V93. 014801 (2004).

[5] “Electron Cloud In the LHC,” (Giovanni.Rumolo@cern.ch and frank.zimmermann@cern.ch <http://ab-abp-rlc.web.cern.ch/ab-abp-rlc-ecloud/>) This site also, lists references to major e-cloud conferences proceedings.

[6] “LHC Design Report – Vol. I”, edited by O. S. Brüning et. al., Chapter-5 in CERN-2004-003-V-1. - Geneva : CERN, 2004.

[7] L. Rossio and O. Brüning, “High Luminosity Large Hadron Collider A description for Eurobean Strategy Preparatory Group,” CERN ATS-2012-236.

[8] G. Rumolo, et. al, “Electron cloud observations in LHC,” IPAC2011 (2011) p 2862

[9] “The SPS as a vacuum test bench for the electron cloud studies with LHC type beams,” G. Arduini et. al., PAC2001 (2001) p 685; “Electron cloud studies and beam scrubbing effect in the SPS,” J.M. Jimenez, et. al., LHC Project Report 634, 2003.

[10] O. Dominguez, et. al, IPAC2012 (2012) p 3105.

[11] G. Rumolo, Private communications (2011).

[12] E. Shaposhnikova, et. al., IPAC2011 (2011) p 211.

[13] T. Bohl, et. al., EPAC98, (1998) p 978.

[14] E. Shaposhnikova and E. Jensen (private communications, 2012).

[15] E. Mahner, T. Kroyer and F. Caspers, *Phys. Rev. ST Accel. Beams* 11, 094401 (2008).

[16] S. Hancock, P. Knaus, M. Lindroos, “Tomographic Measurements of Longitudinal Phase Space Density”, EPAC’98, p 1520; <http://tomograp.web.cern.ch/tomograp/>

[17] Main contributors to the code E-CLOUD were F. Zimmermann, O. Brüning, X.-L. Zhang, G. Rumolo, D. Schulte, and G. Bellodi; E-CLOUD code has been modified by C. M. Bhat in 2011 to handle complex bunch profiles.

[18] G. Iadarola, “Py-Ecloud and buildup simulations at CERN,” this proceedings.

[19] H. Maury, J. G. Contreras and F. Zimmermann, *Phys. Rev. ST Accel. Beams* 15, 051001 (2012).

[20] T. Mauro, (Test-bench measurements on SEY on 316LN_0 Cmm2), (Private communications, 2012).

[21] J. Maclachlan, ESME – longitudinal beam dynamics code. <http://www-ap.fnal.gov/ESME/>

[22] F. Zimmermann, .A Simulation Study of Electron-Cloud Instability and Beam-Induced Multipacting in the LHC, CERN LHC Project Report 95 (1997); O. Brüning, Simulations for the Beam-Induced Electron Cloud in the LHC beam screen with Magnetic Field and Image Charges,. CERN LHC Project Report 158 (1997); G. Rumolo, F. Ruggiero, F. Zimmermann, Simulationm of the electron Cloud Buildup and its Consequences on Heatload, Beam Stability and Diagnostics,. PRST-AB 4, 012801 (2001); F. Zimmermann, .Electron Cloud Simulations: An Update, Proc. Chamonix 2001, CERN-SL-2001-003 DI (2001).

[23] M. A. Furman and V. H. Chaplin, *Phys. Rev. ST Accel. Beams* 9, 034403 (2006).

[24] Water-bag distributions for the beam bunches are known to provide single as well as multi-bunch stability against Landau damping. In this regard this distribution was also tried in our EC simulations (A. Burov, private communications, 2012). We find little difference between BLMpt5 and water-bag bunch profile and EC simulation results.

[25] B. Henrist, N. Hilleret, C. Scheuerlein and M. Taborelli, *Appl. Surf. Sci.* V1.172 (2001) p95-102

- [26] C. M. Bhat and F. Zimmermann, IPAC2011 (2011) p 1879.
- [27] “Flat bunch creation and acceleration: A possible path for the LHC luminosity upgrade” (2009), C. M. Bhat, FERMILAB-CONF-09-243-AD-APC, the *Proceedings of CARE- HHH workshop 2008 Scenarios for the LHC upgrade and FAIR*, CERN), 2009, CERN-2009-004, 2nd July 2009, p 106-114.